

# Multi-vehicle Dynamic Pursuit using Underwater Acoustics

Brooks L. Reed, Josh Leighton, Milica Stojanovic and Franz S. Hover

## Abstract

Marine robots communicating wirelessly is an increasingly attractive means for observing and monitoring the ocean, but acoustic communication remains a major impediment to real-time control. In this paper we address through experiments the capability of acoustics to sustain highly dynamic, multi-agent missions, in particular range-only pursuit in a challenging shallow-water environment. We present in detail results comparing the tracking performance of three different communication configurations, at operating speeds near  $1.5m/s$ . A “lower bound” case with RF wireless communication, a 4-second cycle and no quantization has a tracking bandwidth of  $\approx 0.5rad/s$ . When using full-sized modem packets with negligible quantization and a 23-second cycle time, the tracking bandwidth is  $\approx 0.065rad/s$ . With 13-bit mini-packets, we employ logarithmic quantization to achieve a cycle time of 12 seconds and a tracking bandwidth of  $\approx 0.13rad/s$ . These outcomes show definitively that aggressive dynamic control of multi-agent systems underwater is tractable today.

## I. INTRODUCTION

Marine robots have played an increasing role in ocean operations during recent years, with the proliferation of many commercial platforms and sensors. A major trend is toward tetherless operations, for which each vehicle has to carry its own power source and have a means of wireless communication. Over distances beyond about one hundred meters, underwater communication is almost exclusively accomplished through acoustics. Acoustic communications bring many challenges, however, such as packet loss, low data rates, and delays; Heidemann *et al.* provide a recent review [1]. These undesirable properties of acoustic communication have limited its use in high-performance, real-time tasks. Typical experiments with acoustic modems and vehicles address packet loss rates [2], [3], distributed navigation [4], and command and control of vehicles from ships [5].

If a capability existed, truly dynamic missions of interest would include networked ocean vehicles following a submarine or a marine animal; the latter has been a dream of biologists for decades. Major gaps exist in our understanding of the life cycles of many important marine animals, such as jellyfish [6], sharks [7], [8], lobsters [9], and more. A broader and more challenging problem is monitoring and following a quickly-evolving plume or other oceanic process [10], [11], where distributed measurements must be combined into an estimate, potentially taking into account prior model information [12]. These tasks involve *dynamic feedback control that relies explicitly on acoustic communication*, and fit into the growing field of network-based control [13].

In an effort to lay some groundwork for exploiting advanced algorithms in a real-world ocean application, this paper addresses with experiments an approach for joint estimation and pursuit of a moving target using acoustic communications; see **Figure 1**. Needless to say, the general pursuit problem has held high interest for decades; it is a canonical mission in space and air, on land, and at sea. Probabilistic pursuit-evasion games have been studied extensively in the robotics literature [14], and pursuer and evader dynamics as well as nonlinear estimation are important factors in these algorithms [15], [16]. The effects of communication constraints have not received much attention [17]. These are often addressed indirectly via decentralized approaches that require minimal exchange of information between agents [18]; see [19], [20] for ocean-specific implementations.

There have been some recent experimental works that are related to our pursuit scenario. Perhaps most intriguing is tracking a leopard shark in extremely shallow water, using a single autonomous vehicle with a hydrophone array of  $2.4m$  spread [21]. The system was successful but the shark evidently moved only  $200m$  or so in 48 minutes reported. Bean *et al.* (2007) studied range-based leader-follower regulation with Micro-Modem mini-packets and  $1m/s$  speeds [22], while Brignone *et al.* (2009) study a similar problem with DSPComm modems and two vehicles operating at  $0.7$  and  $3m/s$  [23]. Both works present data from proof-of-concept field trials with mostly straight trajectories. Soares *et al.* (2013) consider a vehicle following two leaders in a triangle formation, with ranges of

B. Reed is in the MIT/WHOI Joint Program in Oceanographic Engineering. J. Leighton and F. Hover are with MIT Department of Mechanical Engineering. {brooksr8, jleight, hover} at mit.edu M. Stojanovic is with the Northeastern University Department of Electrical Engineering. millitsa at ece.neu.edu

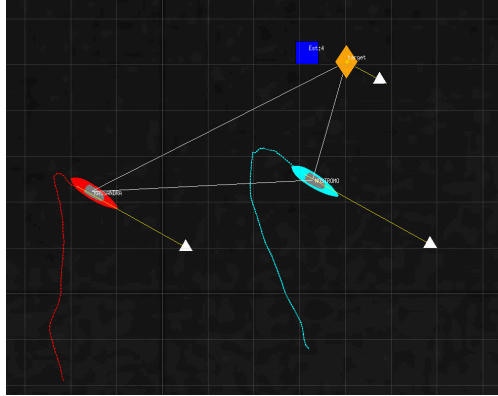


Fig. 1. Screenshot from an active localization and pursuit experiment with acoustic communications. The two vehicles jointly estimate the target location based on range measurements, and move to stay in formation relative to it.

about fifteen meters, speeds around  $0.5m/s$ , and a total loop time of four seconds [24]. In contrast, Cruz *et al.* (2012) consider a complete feedback system—in the sense of two-way communications—for which a stationary controller transmits commands for two mobile followers, who then transmit back their positions [25]. The vehicle speeds are slow, in the neighborhood of  $10cm/s$ , and the cycle time is around twenty seconds. Through analysis, Chen and Pompili (2012) addressed optimization of acoustic communications in coordinated flight of ocean gliders, where currents are especially important [26].

None of these prior works explicitly deal with designing and improving closed-loop frequency response of an integrated multi-vehicle feedback system. This is exactly our objective here. Our design does not rigorously account for stability margins, the multi-rate nature of acoustic communications, inherent geometric nonlinearities, or the fact that autonomous marine vehicles are not ideal actuators. On the other hand, our approach demonstrates practical closed-loop performance at half the Nyquist rate, with little evidence of stability breakdown.

We detail the experiment setup in the following section with descriptions of the vehicles and communication hardware used, the experimental domain, and the estimation and control strategies and parameters. We then give results from three integrated tests, demonstrating the performance achieved.

## II. EXPERIMENTAL SETUP

Our experiment in joint localization and pursuit has two mobile agents sharing sensor information and commands through acoustic links. We make scalar range measurements at each agent, and thus tracking is impossible without their coordination. One agent is designated as the leader that coordinates the measurements and the actions of the followers. This arrangement involves lossy channels at both locations in the feedback loop of **Figure 2**. In the general case, a centralized architecture such as this allows integration with remote sensing, large-scale computations (such as data assimilation), and human-in-the-loop decision-making. The mobile agents attempt to stay close to the target, and in a formation conducive to good sensor performance.

The next five subsections detail the arrangement and operation of this system.

### A. Autonomous Surface Vehicles

We use autonomous kayaks as shown in **Figure 3** for our experiments; they are also described in [27]. Each craft is  $1.8m$  long, weighs about  $40kg$ , and has a rotating thruster near the bow for propulsion and steering. In these tests, the vehicles operate at a nominal speed of  $V = 1.5m/s$ . The relevant navigation sensors available on each vehicle are a tilt-compensated compass and RTK GPS. We use Novotel GPS antennas, uBlox GPS receivers, and the RTKlib software package [28], and have observed position variances on the order of  $10^{-4}m^2$ . Raw compass measurements are passed through a first-order low-pass filter with time constant  $2s$ , and the noise variance on this signal is estimated as  $10deg^2$ .

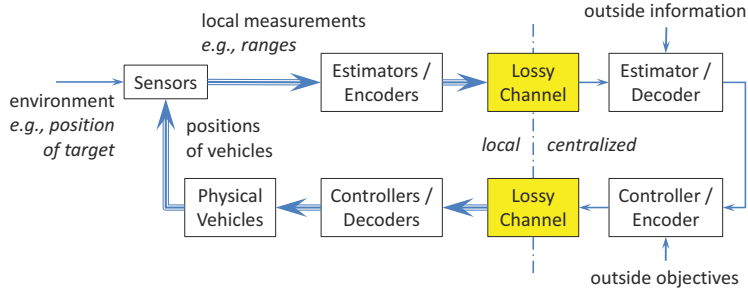


Fig. 2. Block diagram of a generic multi-vehicle feedback system with a centralized estimator and controller, and communication channels at two locations within the loop. Vehicles act as mobile sensors.

The vehicles run MOOS-IvP autonomy software [29] integrated with custom control algorithms and modem interfaces. We rely on the the MOOS heading PID controller, which runs at five Hz, and the MOOS trackline controller, which runs at two Hz. Step response experiments with the kayak under closed-loop heading control indicate a rise time of roughly four seconds, and 30% overshoot; we also note the kayaks are able to turn 180 degrees in approximately three seconds. The MOOS trackline controller is an inner-outer loop that modulates the desired vehicle heading so as to steer it toward a point on the trackline, some lead distance  $l_d$  ahead. When the waypoint is closer than the lead distance, the vehicle simply drives towards the waypoint. For longer distances the result for small errors is a proportional map for desired heading:  $\phi^d \simeq e_x/l_d$ , where  $e_x$  is the cross-track error in meters and  $\phi^d$  is in radians.<sup>1</sup> We set  $l_d = 15m$  for these experiments.

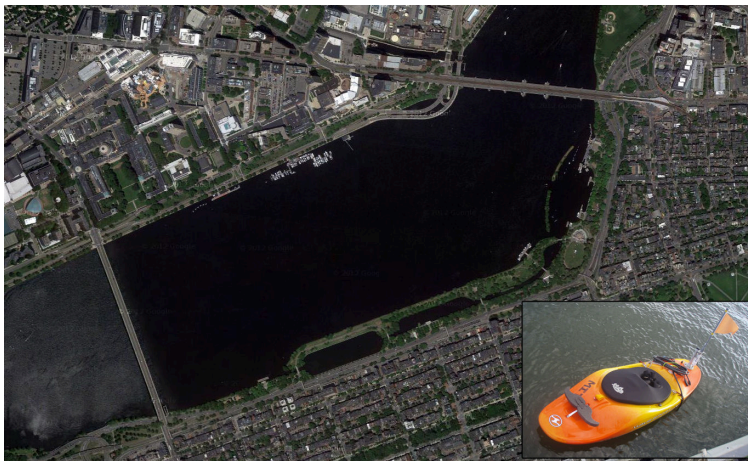


Fig. 3. The Charles River Basin in Cambridge/Boston, MA, and the autonomous kayak Nostromo. Water depth is 2-12m.

### B. Acoustic Communications

We use the the WHOI Micro-Modem [30], a well-established and commercially available technology for underwater acoustic communication. Modems are towed by the vehicles, suspended at a depth of about 1.5 meters; this gives us realistic shallow-water acoustic performance, but with direct access to GPS and RF wireless connectivity at the surface for conducting controlled tests. Along with messaging, we use the modem for one-way travel-time ranging [31]. For messaging, the Micro-Modem has six different packet types with different lengths and data capacities. In this work, we use the FSK mini-packet (“MP”), which is regarded as the most robust of the packet types, but contains only thirteen bits of information. The mini-packets take slightly over one second to transmit. We also use the full-sized Rate 0 FSK packets (“FSK0”), which carry thirty-two bytes of information and take approximately

<sup>1</sup>The linear form written is based on approximation of the tangent function. For errors less than one meter, the MOOS Trackline controller increases the lead distance proportionally, effectively lowering the gain to limit oscillations.

five seconds to transmit. We have observed very large increases in packet loss when using small guard times with both packets, and have found communications to be most reliable with four-second slots for mini-packets and 9.5-second slots for FSK0 packets. All Micro-Modem packets are sent with an acoustic source level of 190 dB rel  $\mu\text{Pa}$ .

The Charles River Basin has fresh water 2-12m deep, a complex bathymetry, and some hard surfaces on the boundaries (seawalls and bridges); our working space is about 1500m long and 500m wide. Acoustic performance in this environment is different from an open-water deep ocean scenario, where multipath and reverberation are much lower, but the ranges are higher. Operations in the Basin can have highly variable acoustic performance, as shown in **Figure 4**. Our conditions are multipath-limited and travel times are short.

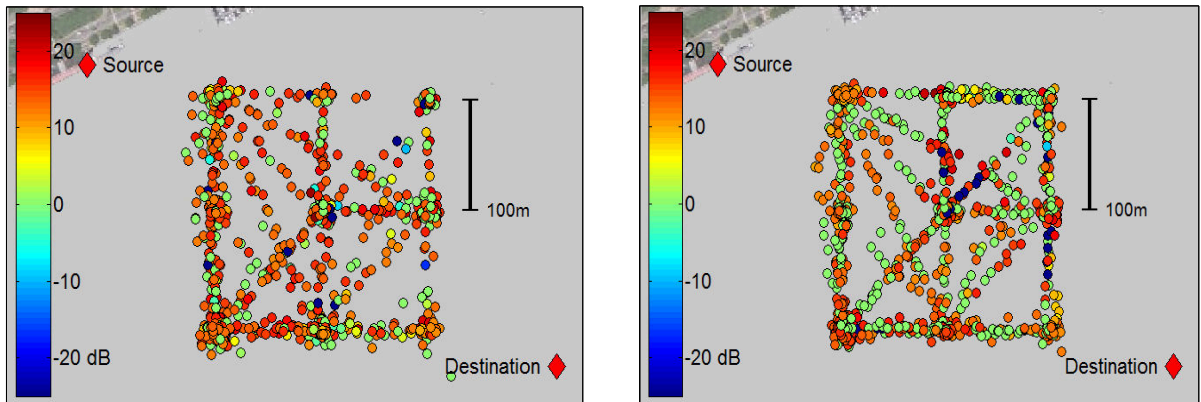


Fig. 4. Micro-Modem performance data in the Charles River Basin, an environment limited by multipath, not power. The left plot shows transmissions from the source to a mobile relay, and the right plot shows transmissions from the relay to the destination. The SNR value indicates sound pressure level relative to ambient noise.

### C. Physical Layout

The two-vehicle pursuit mission encompasses limited communication performance in both the sensing and control channels. In this experiment there is a target to be tracked, “Icarus”, and two cooperating agents “Silvana” and “Nostromo”. We will denote these three nodes with the symbols  $J$ ,  $S$ , and  $N$ , respectively.  $N$  can be thought of as a leader, and  $S$  a follower. The sensing objective is a simple one: to maintain  $S$  and  $N$  in fixed triangular configuration relative to the estimated location of  $J$ , so that measurements will be of high fidelity, *i.e.*, in the sense of a good HDOP [32], and in the sense of a short range. Our pursuit arrangement models the general situation where range or other target sensing degrades with distance, but a high level of tracking precision is desired. Maintaining a close pursuit formation keeps ranges close to a nominal value, allowing for more precise quantization.

An “unstable” situation is encountered if the target crosses the baseline (the line in between the two vehicles acting as a moving long baseline network)—the estimate begins to diverge from the target location. Thus, the disadvantage of a small pursuit formation is that it is easier for the target to cross the baseline, bringing up a tradeoff between robustness of a larger formation and accuracy of a smaller formation (which requires good closed-loop performance).

### D. Cycle Description, Timing and Quantization

We detail the stages of the control loop for the MP and FSK0 cases. Within a cycle step,  $S$  and  $N$  each receive a measurement of range to  $J$  via the Micro-Modems in ranging mode. After a guard period,  $S$  transmits its current location and range data to  $N$  through acoustic communication.  $N$  combines this information with its own location and range information to generate an estimated location of  $J$ .  $N$  calculates control actions for itself and for  $S$ , and transmits the latter back to  $S$ . The cycle includes three separate transmissions and there are no acknowledgments. We enforce the fixed time slots with a number of timeouts, as indicated in **Figure 5**. We synchronize clocks using the network time protocol; in the absence of clock synchronization, we note that precision clocks are becoming increasingly practical for use on underwater vehicles [31].

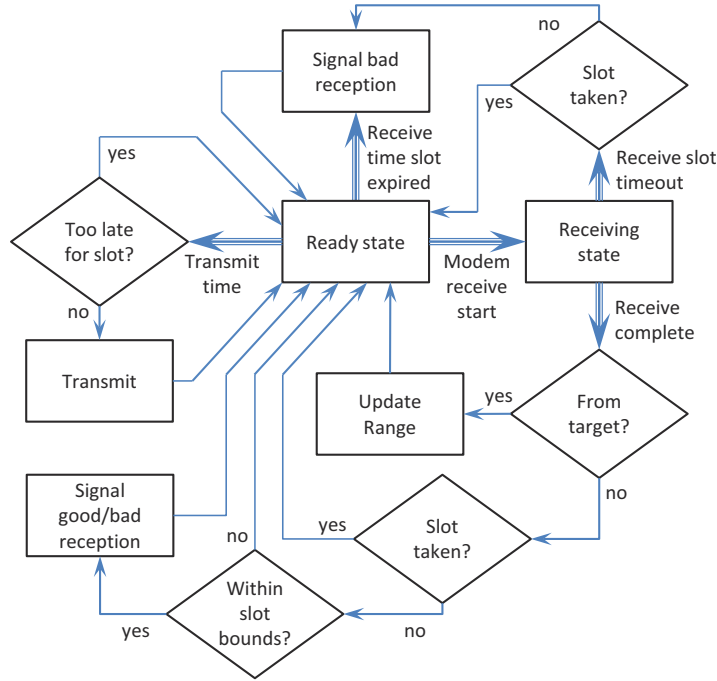


Fig. 5. The internal state machine used on each vehicle to maintain consistent timing with respect to predefined transmission and reception slots. Thick arrows distinguish acoustic events that initiate state changes or other actions from normal logic flow. Special operations are indicated to handle detection of erroneous multipath receptions, which frequently occur in this environment. For example, a good reception for a time slot  $T_i$  will follow the “Receive complete” path (bottom) to a good signal. A trailing multipath reception will return to the receiving state, but the end of time slot  $T_i$  will arrive before the end of the packet. In the top right, slot  $T_i$  is already taken by the good reception, so we return to the ready state with no action taken.

For feedback control, there is a problem-dependent tradeoff to be made between time-averaged throughput (usually achieved with long coding blocks) and timeliness of the information (shorter messages). We present data using both 13-bit mini-packets and 32-byte FSK0 packets as an initial study of this tradeoff. The MP scenario minimizes cycle time at the expense of data quantization; we achieved a total cycle time of 12 seconds in this configuration.<sup>2</sup> With the FSK0 configuration, packets require no quantization for the data types we send, but do require a 9.5sec time slot for each transmission, resulting in a total cycle time of 23 seconds.<sup>3</sup> The “wifi” scenario involves a 4s slot for acoustic ranging, as detailed above. However, the inter-vehicle communications are handled instantaneously via wifi, so the estimate is available immediately upon reception of ranges.

For the message from  $S$  to  $N$  in the MP case, we used three bits for the range, and five bits each direction for  $S$ 's location in a  $32 \times 32$  discretized workspace; this workspace had ten-meter resolution. The range data were logarithmically quantized relative to a desired range of 50m, with seven bin edges located at [19.2 32.5 42.5 50 57.5 67.5 80.8]m, and the three-bit messages decoded as [11.5 26.8 38.2 46.8 53.2 61.8 73.2 88.5]m. This correlates with the density  $\rho = 0.75$  [33]. For the message from  $N$  back to  $S$ , we used five bits in each of  $x$  and  $y$  for the desired location in the workspace. This left three bits unused. Note that with quantization, there is a tradeoff between range and precision. With this choice, any range larger than 80.8m is decoded as the furthest range bin, so when ranges are very large, estimation suffers. Increasing this outer range would come at the expense of resolution of the bins near the 50m nominal range; it is the control system's job to keep the vehicles in the desired formation so that small bins can be used.

<sup>2</sup>When range measurements do not interfere with modem packets and the cycle consists of just two-way communications (e.g. using GPS and wifi for ranges), we have achieved a six-second total cycle time with mini-packets in the field.

<sup>3</sup>As we were submitting this paper we became aware of several modifications in the operation of the Micro-Modems that likely will allow for slightly faster cycle times.

### E. Settings and User Choices

The tracking system contains a nonlinear sigma-point filter (SPF) [34], well-suited for this type of application.<sup>4</sup> The nonholonomic target  $\mathcal{J}$  (a small motorboat) was assumed to be moving at constant  $1.55m/s$ , with stochastic low-pass, zero-mean turning rate with variance  $Q$ . The observation vector contains the two noisy ranges, with variances  $R_S$  and  $R_N$  for range measurements to Silvana and Nostromo, respectively. The sensor noise for range measurements was chosen based on prior characterizations of the WHOI Micro-Modem ranging capability [30], [36] and our own observed LBL performance. The sensor noise for the follower range measurement ( $\mathcal{J}$  to  $\mathcal{S}$ ) in the MP experiment was set to a higher value to account for the effects of quantization during communication of the measurement from  $\mathcal{S}$  to the filter running on  $\mathcal{N}$ . Settings for the three configurations are given in **Table I**.

When a measurement is not available (either due to a missed LBL range, or a dropped measurement packet from  $\mathcal{S}$  to  $\mathcal{N}$ ), we take the standard approach of setting the noise of the lost measurement to infinity [37]. In the MP and FSK0 configurations, when a control command from  $\mathcal{N}$  to  $\mathcal{S}$  is dropped, the previously-received command for  $\mathcal{S}$  remains the desired waypoint. This approach is chosen to ensure safe operation in the case of many missed packets. In the MP case, three bits are left unused in the command packet which could encode contingency plans.

The desired observation triangle has a sixty-degree vertex at  $\mathcal{J}$ . For the MP and wifi cases, the ranges to each of  $\mathcal{S}$  and  $\mathcal{N}$  were  $50m$ ; for the FSK0 case the desired ranges were  $100m$  due to the slower cycle time.<sup>5</sup>

TABLE I  
SETTINGS AND RESULTS FOR THE THREE CONFIGURATIONS. DESRANGE IS THE LENGTH OF THE LEGS IN THE DESIRED SENSING FORMATION. THE COLUMNS WITH  $R$  ARE THE SENSOR NOISE VARIANCES FOR THE RANGE MEASUREMENTS TO EACH VEHICLE.  $Q$  IS THE TARGET HEADING RATE VARIANCE. BW IS THE CLOSED-LOOP TRACKING BANDWIDTH, AND ATTEN IS THE TRACKING ERROR ATTENUATION AT  $0.065rad/s$ . ALSO SEE **Figure 9**.

Config	Cycle Time <i>sec</i>	DesRange <i>m</i>	$R_S$ $m^2$	$R_N$ $m^2$	$Q$ $(rad/s)^2$	BW <i>rad/s</i>	Atten <i>dB</i>
FSK0	23	100	0.25	0.25	0.01	0.065	0
Wifi	4	50	0.25	0.25	0.05	0.5	18
MP	12	50	0.25	9	0.05	0.13	7

### III. EXPERIMENTAL RESULTS

We compare the tracking performance of three different communication configurations: full-sized packets (“FSK0”) with negligible quantization and a  $23s$  cycle, RF wireless communication (“wifi”) with a  $4s$  cycle, and 13-bit mini-packets (“MP”) with a  $12s$  cycle. The “wifi” configuration roughly represents a single vehicle towing a long two-element array, as inter-vehicle communication is lossless and immediate. However, a true “single-vehicle with array” would be less maneuverable than vehicles without arrays, and could not pursue the target as closely without risking the target crossing the baseline. For close pursuit with multiple vehicles, we can view the “wifi” case as a lower bound on performance.

The experiments we report were conducted on 8-9 July 2013, both days with light winds.<sup>6</sup> **Figures 6, 7, 8** give results from the FSK0, wifi and MP tests, respectively. In each test,  $\mathcal{J}$  moved in a largely random trajectory, as shown in the birds-eye view in the upper left (Subplot **a**) and the time traces in Subplot **c**. The upper right (Subplot **b**) shows the sensing formation every fifteen time steps; we see that while the ideal triangle configuration was rarely achieved in the FSK0 and MP tests, the target did not cross the baseline (the red straight line between the two nodes acting as a moving LBL network), nor did the geometry ever stay poor for a sustained period. The tracking and pursuit system did not lose the target.

The measured ranges are reported in Subplot **e** in each figure, including quantization of raw values sent to  $\mathcal{N}$  from  $\mathcal{S}$  in the subsequent measurement packet for the MP case. Range losses in all cases are low, as the Micro-Modem ranging ping is fairly robust; see figure captions for loss statistics. Subplot **d** shows the north and east tracking error

<sup>4</sup>Other nonlinear, range-only filters, such as particle filters, could also be used [35].

<sup>5</sup>The ranges are set relative to the distance the target can drive in a time step, so that the target is unlikely to cross the baseline before the control system can react.

<sup>6</sup>This data set, along with videos, is publicly available at <http://web.mit.edu/hovergroup/resources.html>.

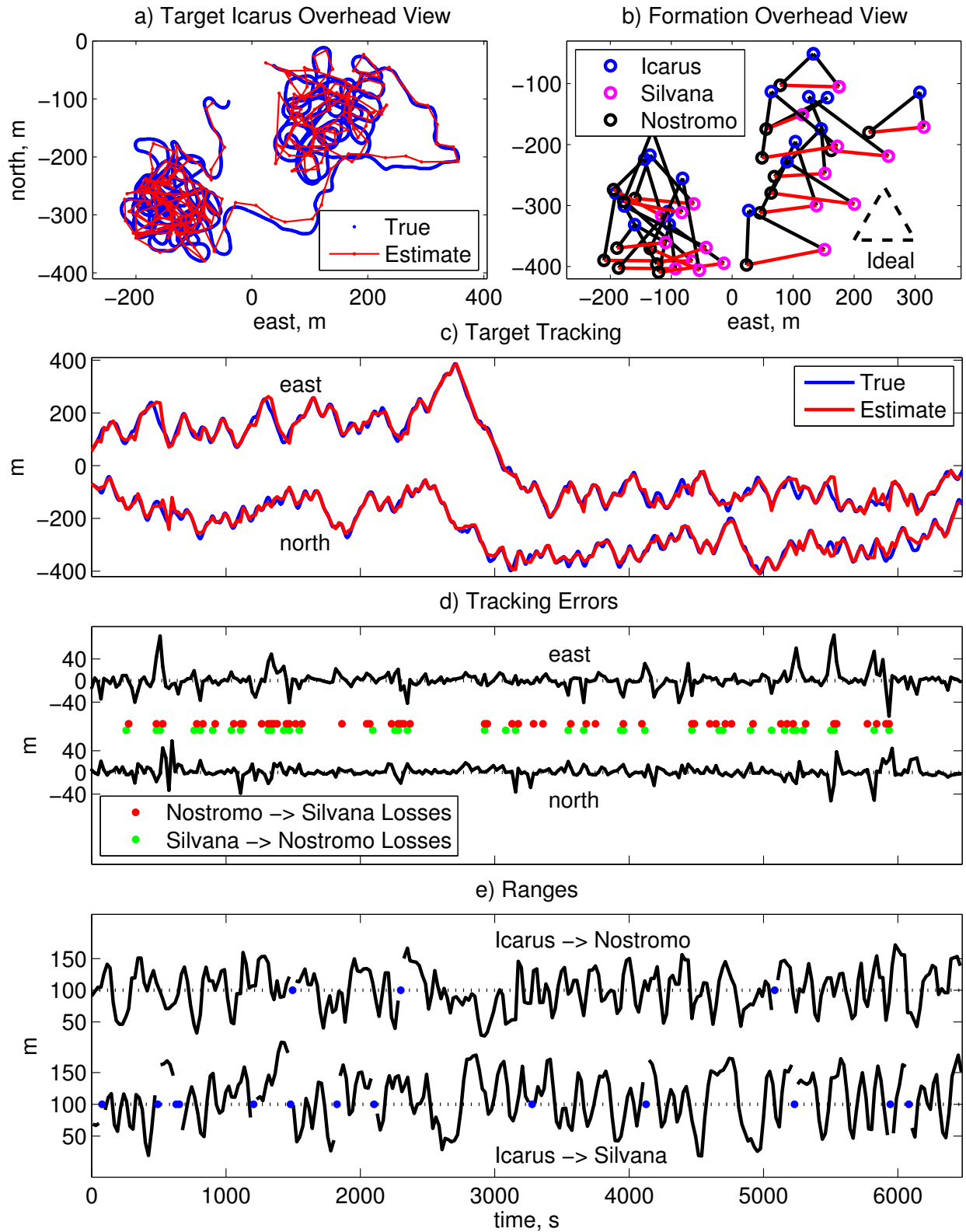


Fig. 6. FSK0 test results (6463 seconds, 281 cycles). a) Overview of true and estimated trajectories of the target Icarus. b) Sensing formation every 15 time steps. c) Actual (GPS) and estimated trajectory of target Icarus. d) Estimation error of Icarus' location. The RMS radius of estimation errors was 20.2m. Data packet losses are also shown; loss rates were:  $\mathcal{N} \rightarrow \mathcal{S} = 19.9\%$ ,  $\mathcal{S} \rightarrow \mathcal{N} = 14.0\%$ . e) Range measurements from Icarus to each kayak, and losses. Range loss rates were:  $\mathcal{J} \rightarrow \mathcal{N} = 1.1\%$ ,  $\mathcal{J} \rightarrow \mathcal{S} = 4.8\%$ .

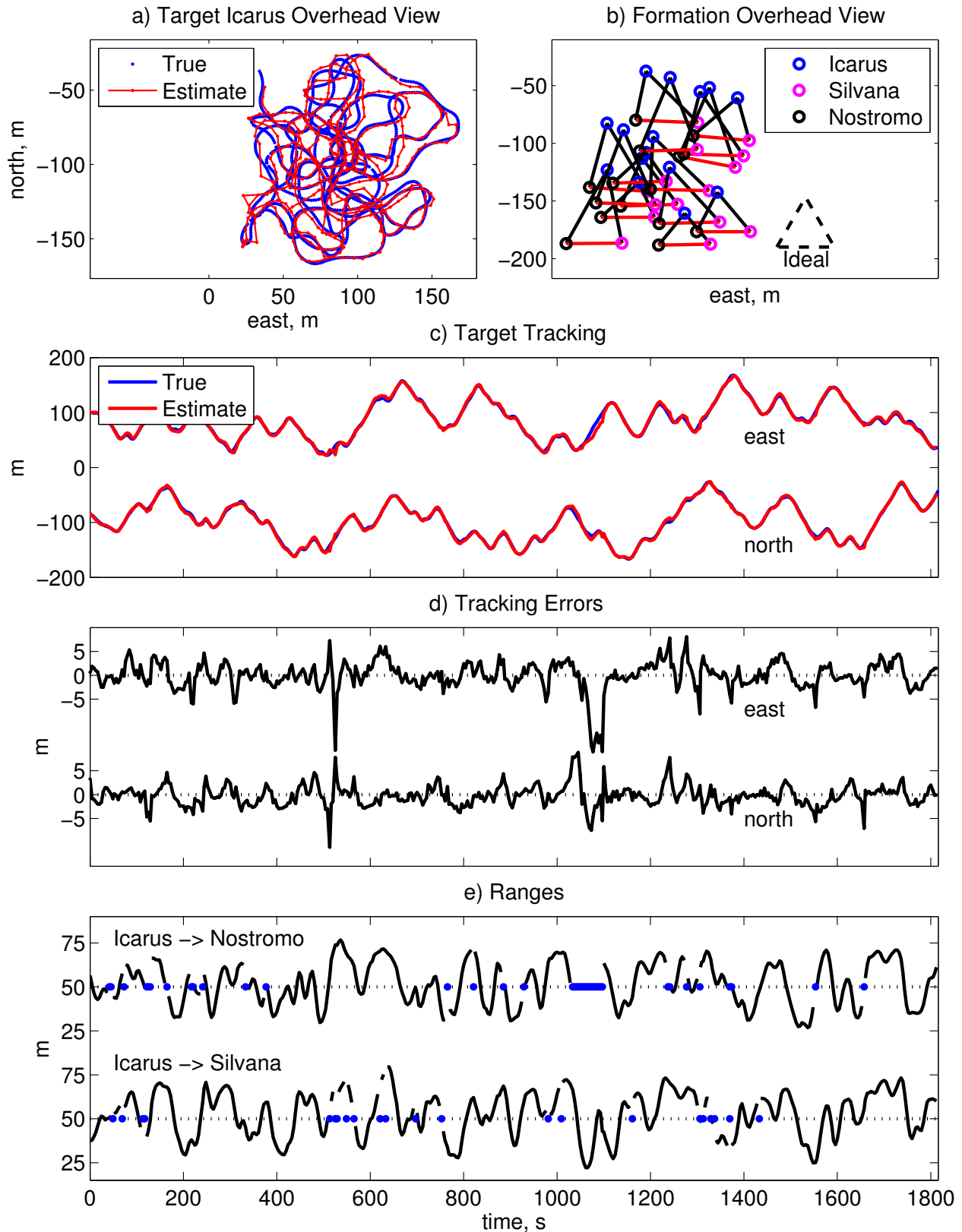


Fig. 7. Wifi test results (1820 seconds, 455 cycles). a) Overview of the true and estimated trajectories of the target Icarus. b) Sensing formation every 30 time steps. c) Actual (GPS) and estimated trajectory of the target Icarus. d) Estimation error of Icarus' location. The RMS radius of estimation errors was  $3.8m$ . e) Range measurements from Icarus to each vehicle, and losses. Range loss rates were:  $J \rightarrow N = 9.0\%$ ,  $J \rightarrow S = 4.8\%$ .



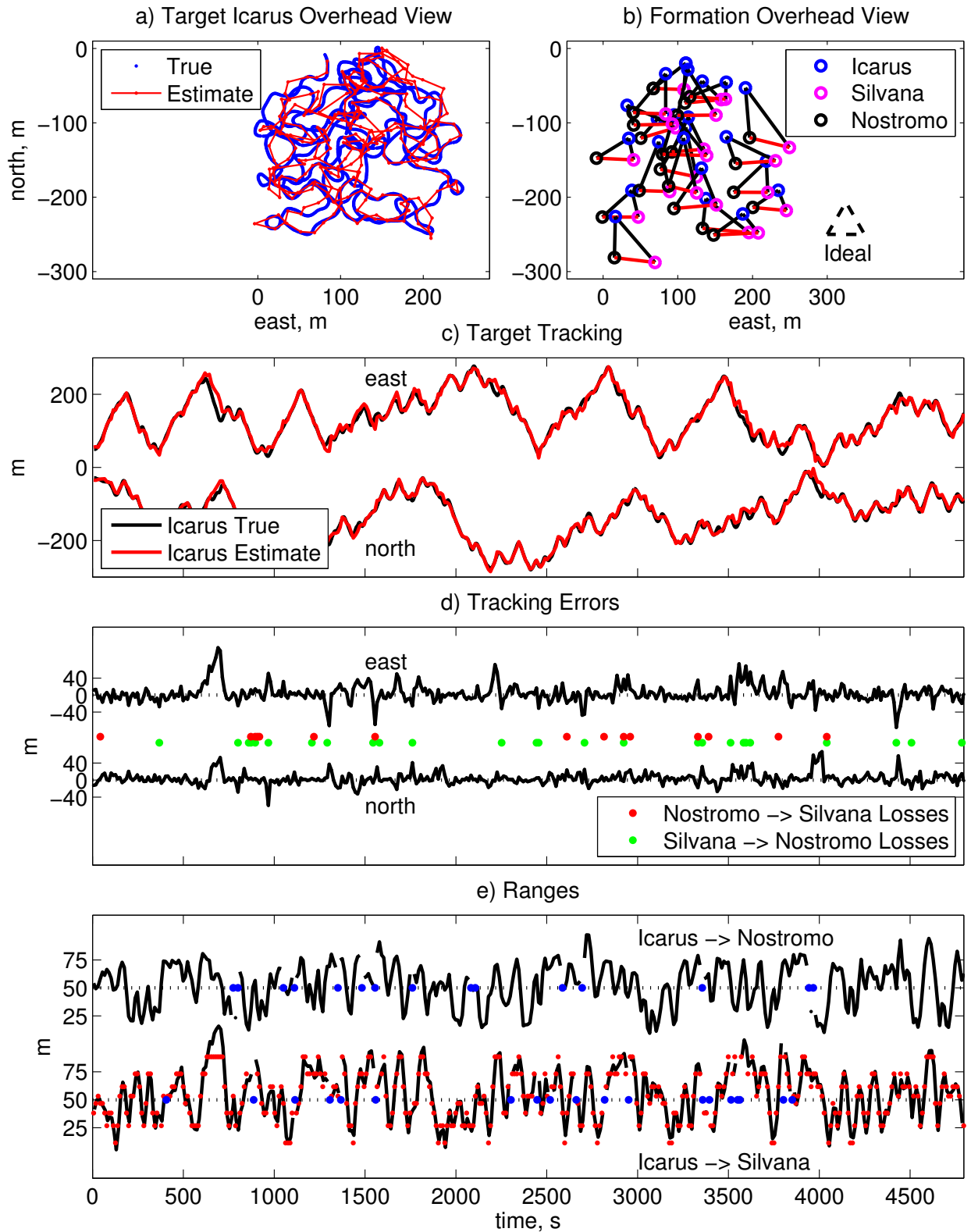


Fig. 8. MP test results (4800 seconds, 400 cycles). a) Overview of the true and estimated trajectories of the target Icarus. b) Sensing formation every 15 time steps. c) Actual (GPS) and estimated trajectory of the target Icarus. d) Estimation error of Icarus' location. The RMS radius of estimation errors was  $12.7m$ . Data packet losses are also shown; the loss rates were:  $N \rightarrow S = 3.8\%$ ,  $S \rightarrow N = 6.5\%$ . e) Range measurements from Icarus to each vehicle, and losses. Range loss rates were:  $J \rightarrow N = 3.8\%$ ,  $J \rightarrow S = 4.8\%$ . Quantized measurements sent from Silvana to Nostromo are shown in red on top of the true measured ranges.

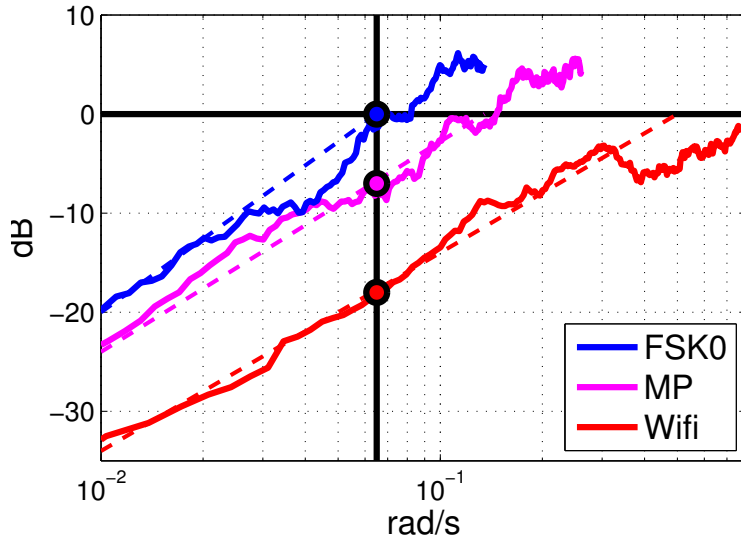


Fig. 9. Empirical FFT-based transfer function for estimator error divided by target motion. The solid lines show the mean of the X and Y spectra. The dashed lines show an approximate linear fit for low-frequency attenuation. Dots show the approximate attenuation at  $0.065\text{rad/s}$ .

over time, along with dropped communication packets for the MP and FSK cases. The packet losses are significantly higher for the FSK0 test. Most of the larger errors occur following packet losses, but some large spikes (such as around 500 seconds in the mini-packet test) are not near packet losses—errors can also occur due to poor sensing geometry, and in the MP case, quantization.

Recalling our broad objective to achieve dynamic control through mobile acoustic networks, it is revealing to ask what is the effective closed-loop estimation bandwidth achieved. A direct FFT-based empirical transfer function for the estimation error divided by target motion is shown for each test in **Figure 9**; spectra have been smoothed with a 5-point centered moving average. The FSK0 test has a break frequency for tracking the motion of  $J$  at approximately  $0.065\text{rad/s}$ , slightly less than half the Nyquist rate for the twenty-three-second cycle. The wifi test has a break frequency of approximately  $0.5\text{rad/s}$ . The MP test has a break frequency of approximately  $0.13\text{rad/s}$ . We can also compare the attenuation of tracking error for each configuration at  $0.065\text{rad/s}$ . FSK0 has zero attenuation, wifi has 18 dB attenuation, and MP has 7 dB.

#### IV. CONCLUSION

Our experiment has achieved aggressive target pursuit in the underwater environment. As opposed to a traditional control and estimation design scenario, the mission here is accomplished through a highly integrated vehicle system performing full joint estimation and coordination through lossy acoustic communications underwater. The three experimental configurations studied show the effects of cycle time, quantization, and acoms performance on the frequency response of the system. In particular, the MP and FSK0 experiments demonstrate that for tracking highly dynamic targets it is beneficial to trade-off quantization for low cycle time.

More broadly, the pursuit mission presented in this paper is one special case of a much larger picture; we believe that undersea communications and coordinated control will soon enable truly distributed and dynamic tracking of moving ocean features, such as eddies, plumes and fronts. Such vehicle systems would be able to observe important chemical, biological, and physical processes over larger physical scales than a single vehicle can cover, and would interface with observation systems on land and in the atmosphere, as well as with humans. Operations like this – “oceanographic pursuit” – are a natural progression of marine technology toward the group autonomy and dynamic behavior that we have seen developed already in the terrestrial environment and in the air [38]. Specification of physical configurations, scheduling, routing, and multi-rate control design will undoubtedly join the mix, making underwater pursuit a rich problem for future work.

## ACKNOWLEDGMENTS

Work is supported by the Office of Naval Research, Grant N00014-09-1-0700, the National Science Foundation, Contract CNS-1212597, and the Finmeccanica Career Development Professorship. We thank Mei Cheung for providing Figure 4 and help with experimental implementation. We thank Toby Schneider and Mike Benjamin at MIT, and Keenan Ball and Sandipa Singh at WHOI, for their help on technical items. We also acknowledge MIT Sailing Master Fran Charles.

## REFERENCES

- [1] J. Heidemann, M. Stojanovic, and M. Zorzi, "Underwater sensor networks: applications, advances and challenges," *Philosophical Transactions of the Royal Society A: Mathematical, Physical and Engineering Sciences*, vol. 370, no. 1958, pp. 158–175, 2012.
- [2] A. Caiti, V. Calabro, G. Dini, A. Duca, and A. Munafa, "AUVs as mobile nodes in acoustic communication networks: Field experience at the UAN10 experiments," in *Proc. MTS/IEEE OCEANS*, 2011.
- [3] J. Canning, M. Anderson, D. Edwards, M. O'Rourke, T. Bean, J. Pentzer, and D. Odell, "A low bandwidth acoustic communication strategy for supporting collaborative behaviors in a fleet of autonomous underwater vehicles," *US Navy J. Underwater Acoustics*, 2009.
- [4] A. Bahr, J. Leonard, and M. Fallon, "Cooperative localization for autonomous underwater vehicles," *International J. Robotics Research*, vol. 28, no. 6, p. 714, 2009.
- [5] T. Schneider and H. Schmidt, "Unified command and control for heterogeneous marine sensing networks," *Journal of Field Robotics*, vol. 27, no. 6, pp. 876–889, 2010.
- [6] J. Rife and S. Rock, "Design and validation of a robotic control law for observation of deep-ocean jellyfish," *IEEE Trans. Robotics*, vol. 22, no. 2, pp. 282–291, april 2006.
- [7] G. Skomal and G. Benz, "Ultrasonic tracking of greenland sharks, somniosus microcephalus, under arctic ice," *Marine Biology*, vol. 145, no. 3, pp. 489–498, 2004.
- [8] F. Voegeli, M. Smale, D. Webber, Y. Andrade, and R. O'Dor, "Ultrasonic telemetry, tracking and automated monitoring technology for sharks," *Environmental Biology of Fishes*, vol. 60, no. 1, pp. 267–282, 2001.
- [9] I. Vázquez-Rowe, D. Iribarren, M. T. Moreira, and G. Feijoo, "Combined application of life cycle assessment and data envelopment analysis as a methodological approach for the assessment of fisheries," *The International Journal of Life Cycle Assessment*, vol. 15, no. 3, pp. 272–283, 2010.
- [10] R. Camilli, C. Reddy, D. Yoerger, B. Van Mooy, M. Jakuba, J. Kinsey, C. McIntyre, S. Sylva, and J. Maloney, "Tracking hydrocarbon plume transport and biodegradation at Deepwater Horizon," *Science*, vol. 330, no. 6001, p. 201, 2010.
- [11] J. Farrell, S. Pang, W. Li, and R. Arrieta, "Chemical plume tracing experimental results with a REMUS AUV," in *Proc. MTS/IEEE OCEANS*, vol. 2. IEEE, 2003, pp. 962–968.
- [12] N. Leonard, D. Paley, F. Lekien, R. Sepulchre, D. Fratantoni, and R. Davis, "Collective motion, sensor networks, and ocean sampling," *Proc. IEEE*, vol. 95, no. 1, pp. 48–74, 2007.
- [13] J. Baillieul and P. Antsaklis, "Control and communication challenges in networked real-time systems," *Proc. of the IEEE*, vol. 95, no. 1, pp. 9–28, 2007.
- [14] R. Vidal, O. Shakernia, H. Kim, D. Shim, and S. Sastry, "Probabilistic pursuit-evasion games: theory, implementation, and experimental evaluation," *IEEE Trans. Robotics and Automation*, vol. 18, no. 5, pp. 662–669, oct 2002.
- [15] E. Liao, G. Hollinger, J. Djughash, and S. Singh, "Preliminary results in tracking mobile targets using range sensors from multiple robots," *Distributed Autonomous Robotic Systems 7*, pp. 125–134, 2006.
- [16] K. Zhou and S. Roumeliotis, "Optimal motion strategies for range-only constrained multisensor target tracking," *IEEE Trans. Robotics*, vol. 24, no. 5, pp. 1168–1185, 2008.
- [17] Y. Mostofi, T. Chung, R. Murray, and J. Burdick, "Communication and sensing trade-offs in decentralized mobile sensor networks: a cross-layer design approach," in *Proc. 4th International Symposium on Information Processing in Sensor Networks*. IEEE Press, 2005, p. 16.
- [18] T. Chung, J. Burdick, and R. Murray, "A decentralized motion coordination strategy for dynamic target tracking," in *Proc. IEEE International Conference on Robotics and Automation*, 2006, pp. 2416–2422.
- [19] A. Gadre, D. Maczka, D. Spinello, B. McCarter, D. Stilwell, W. Neu, M. Roan, and J. Hennage, "Cooperative localization of an acoustic source using towed hydrophone arrays," in *Proc. IEEE/OES Autonomous Underwater Vehicles*, oct. 2008, pp. 1–8.
- [20] D. Eickstedt, M. Benjamin, H. Schmidt, and J. Leonard, "Adaptive tracking of underwater targets with autonomous sensor networks," *US Navy J. Underwater Acoustics*, vol. 56, pp. 465–495, 2006.
- [21] C. M. Clark, C. Forney, E. Manii, D. Shinzaki, C. Gage, M. Farris, C. G. Lowe, and M. Moline, "Tracking and following a tagged leopard shark with an autonomous underwater vehicle," *Journal of Field Robotics*, vol. 30 (3), pp. 309–322, 2013.
- [22] T. Bean, J. Canning, G. Beidler, M. O'Rourke, and D. Edwards, "Designing and implementing collaborative behaviors for autonomous underwater vehicles," in *Proc. International Symposium on Unmanned Untethered Submersible Technology*, 2007.
- [23] L. Brignone, J. Alves, and J. Opderbecke, "GREX sea trials: first experiences in multiple underwater vehicle coordination based on acoustic communication," in *Proc. MTS/IEEE OCEANS*, 2009.
- [24] J. Soares, A. Aguiar, A. Pascoal, and A. Martinoli, "Joint ASV/AUV range-based formation control: Theory and experimental results," in *Proc. International Conf. Robotics and Automation (ICRA)*, 2013.
- [25] N. A. Cruz, B. M. Ferreira, A. C. Matos, C. Petrioli, R. Petroccia, and D. Spaccini, "Implementation of an underwater acoustic network using multiple heterogeneous vehicles," in *Proc. MTS/IEEE Oceans*. IEEE, 2012, pp. 1–10.
- [26] B. Chen and D. Pompili, "Team formation and steering algorithms for underwater gliders using acoustic communications," *Computer Communications*, vol. 35, no. 9, pp. 1017–1028, 2012.
- [27] E. Gilbertson, B. Reed, J. Leighton, M. Cheung, and F. Hover, "Experiments in dynamic control of autonomous marine vehicles using acoustic modems," in *Proc. IEEE International Conf. on Robotics and Automation*, 2013.
- [28] T. Takasu and A. Yasuda, "Development of the low-cost RTK-GPS receiver with an open source program package RTKLIB," in *International Symposium on GPS/GNSS, International Convention Center Jeju, Korea*, 2009.

- [29] M. Benjamin, J. Leonard, H. Schmidt, and P. Newman, "An overview of MOOS-IvP and a brief users guide to the IvP helm autonomy software," *Massachusetts Institute of Technology, MIT CSAIL, Tech. Rep. TR-2009-28-07*, 2009.
- [30] L. Freitag, M. Grund, S. Singh, J. Partan, P. Koski, and K. Ball, "The WHOI Micro-Modem: An acoustic communications and navigation system for multiple platforms," in *Proc. MTS/IEEE OCEANS*, 2005.
- [31] R. M. Eustice, H. Singh, and L. L. Whitcomb, "Synchronous-clock one-way-travel-time acoustic navigation for underwater vehicles," *J. Field Robotics, Special Issue on State of the Art in Maritime Autonomous Surface and Underwater Vehicles*, vol. 28, no. 1, pp. 121–136, 2011.
- [32] B. Bingham, "Predicting the navigation performance of underwater vehicles," in *Proc. IEEE/RSJ Intelligent Robots and Systems*, 2009, 2009.
- [33] M. Fu and L. Xie, "The sector bound approach to quantized feedback control," *IEEE Trans. Automatic Control*, vol. 50, no. 11, pp. 1698 – 1711, nov. 2005.
- [34] S. Julier and J. Uhlmann, "New extension of the Kalman filter to nonlinear systems," in *AeroSense'97. International Society for Optics and Photonics*, 1997, pp. 182–193.
- [35] F. Dellaert, D. Fox, W. Burgard, and S. Thrun, "Monte carlo localization for mobile robots," in *Robotics and Automation, 1999. Proceedings. 1999 IEEE International Conference on*, vol. 2. IEEE, 1999, pp. 1322–1328.
- [36] J. Curcio, J. Leonard, J. Vaganay, A. Patrikalakis, A. Bahr, D. Battle, H. Schmidt, and M. Grund, "Experiments in moving baseline navigation using autonomous surface craft," in *Proc. MTS/IEEE OCEANS*, 2005.
- [37] B. Sinopoli, L. Schenato, M. Franceschetti, K. Poolla, M. Jordan, and S. Sastry, "Kalman filtering with intermittent observations," *IEEE Trans. Automatic Control*, vol. 49, no. 9, pp. 1453–1464, 2004.
- [38] M. Dunbabin and L. Marques, "Robots for environmental monitoring: Significant advancements and applications," *Robotics & Automation Magazine, IEEE*, vol. 19, no. 1, pp. 24–39, 2012.